Pavel NOVOTNÝ
Václav PÍŠTĚK
Jiří STODOLA

# VIRTUAL ENGINE - A TOOL
# FOR MILITARY TRUCK RELIABILITY INCREASE

Reviewer: Františka PEŠLOVÁ

A b s t r a c t :

*The internal combustion engine development process requires CAE models which yield results for the concept phase at a very early stage and which can be further detailed on the same program platform as the development process progresses. The vibratory and acoustic behavior of the powertrain is highly complex, consisting of many components that are subject to loads that vary greatly in magnitude and which operate at a wide range of speeds. The interaction of the crank and crankcase is a major problem that powertrain designers have to face when optimizing the vibration and noise characteristics of the powertrain. The Finite Element Method (FEM) and Multi-Body Systems (MBS) are suitable for the creation of 3-D calculation models. Non-contact measurements enable complex calculation models to be verified. All numerical simulations and measurements are performed on an in-line six-cylinder diesel engine.*

## 1. Introduction

Manufacturers in the military automotive industry are constantly looking for ways to maintain their competitiveness by getting innovative products to market first. Plus,

safety issues, fuel efficiency, warranty costs, styling and other goals place increased demands and expectations on the military automotive industry to develop high-quality products. Pressures to meet these stringent requirements while reducing product development cycle time on the order of 50 percent represent a huge challenge to researches, suppliers, co-development partners and others in the military automotive value chain. Time-to-market is critical, because the value of innovation will be lost if competitors win the race to the showroom floor with similar designs. A few weeks' delay can result in millions of dollars in lost revenue, and the first company reaching the market typically gets million shares of sales. As a result, more and more manufacturers are discovering that the only way to achieve development goals is to employ engineering simulation technologies. This goal can only be achieved by increasing the amount of simulation. All major military truck producers, as well as companies in a wide range of other manufacturing industries, are using virtual prototyping to evaluate designs through computer simulation and analysis, thereby reducing their reliance on hardware testing. The aim is not to entirely eliminate such testing, but rather to reduce the number of cycles and guide the empirical procedure towards verifying well-defined performance attributes. By studying product configurations in the early phases of development, engineers can make changes and refine designs easily and inexpensively. Studies have shown that the cost of change increases exponentially with each stage of development, thus making changes costly during detailed design, very expensive during prototype testing and tremendously high during production. Moreover, correcting errors after the product is sold can be prohibitive in terms of recall and warranty costs, sometimes causing economically catastrophic consequences for manufacturers. One of the greatest benefits of simulation early in development is that engineers have the time and technology to evaluate alternatives, run "what-if" scenarios and come up with innovative designs. In a major push to accelerate its product development cycle, one major automaker implemented a concerted front-end loading initiative involving the use of early simulation in conjunction with other process changes and slashed development time and cost including the number of full physical prototypes by between 30 and 40 percent.

## 2. Modeling approach

### 2.1. CAE Modeling

For complex simulation processes and high-quality products such as combustion engines, higher effort is necessarily required for simulation and modeling. The development process starts with Computer Aid Design (CAD). For the cranktrain dynamics CAD models give basic geometric information about engine parts and can be used for the creation of FE models (e.g. crankshafts or engine blocks) or MBS rigid parts (e.g. pistons or piston pins) [2]. **Figure 1** shows a CAD model of an in-line six-cylinder diesel engine cranktrain.
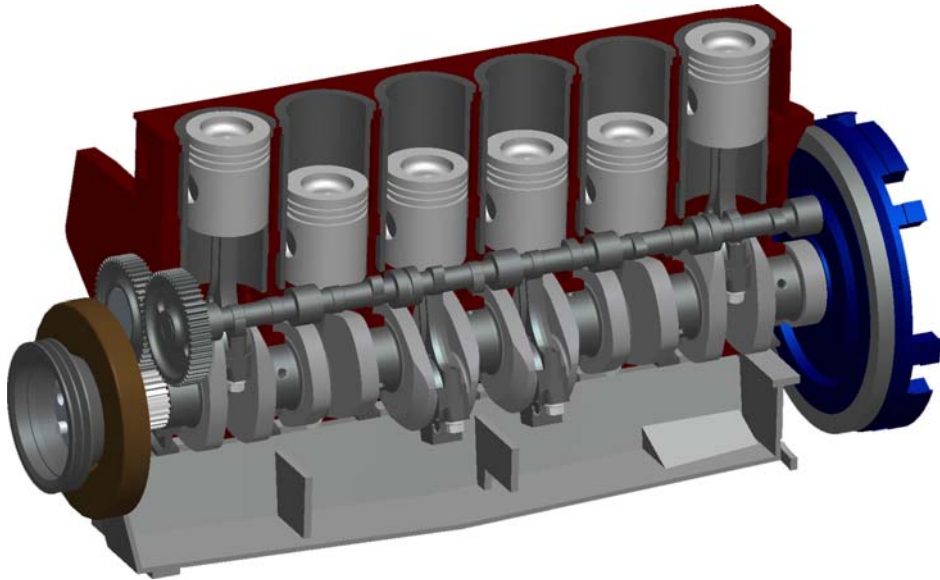
**Figure 1** Diesel in-line six-cylinder engine CAD models

In the powertrain development process, several numeric simulation techniques have steadily gained in importance. In the case of dynamic structural calculations the Finite Element Method (FEM) is state of the art.

In many cases the FE models are suitable for dynamic calculation such as modal analysis or harmonic analysis, but the durability of the product requires a different FE modeling approach. Frequently dynamic models have also been simplified to remove details such as holes and fillets which play an important role in the durability of the product. FE model of in-line six-cylinder crankshaft includes small geometric details and is suitable for a stress-strain analysis as well as a fatigue analysis. For realistic calculations the model of a FE block must be attached but the FE model of an engine block is used for modal analysis and for stiffness calculations. It therefore has a uniform hexa element mesh. Figure 2 presents a detailed FE model of an in-line six-cylinder crankshaft.
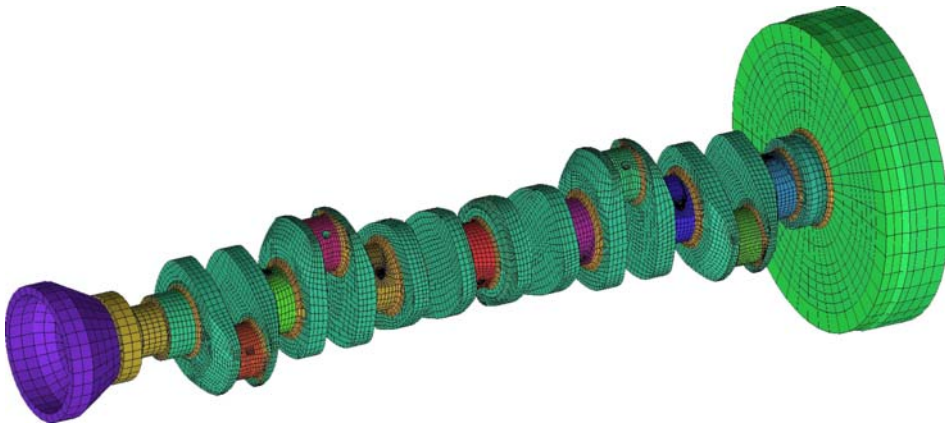
**Figure 2** Diesel in-line six-cylinder engine FE model

Complex computational models of powertrain are assembled in Multi-Body System (MBS) ADAMS. MBS enables the creation of virtual prototypes, realistically simulating the full-motion behavior of complex mechanical systems on computers and quickly analyzing multiple design variations until an optimal design is achieved. This reduces the number of costly physical prototypes, improves design quality, and dramatically shortens product development time.

One drawback of the MBS program is that all components are assumed to be rigid [5]. In the ADAMS program, tools to model component flexibility exist for geometrically simple structures only. To account for the flexibility of a geometrically complex component, ADAMS relies on data transferred from finite-element programs such as ANSYS.

The flexibility of a geometrically complex component, such as a crankshaft, is represented by a matrix that is stored in modal neutral file (.MNF) created by a FE program.

The algorithm used to create the modal neutral file is based on a formulation called component mode synthesis (also known as dynamic substructuring). ADAMS uses the approach of Craig Bampton with some slight modifications. According to this theory, the motion of a flexible component with interface points is spanned by the interface constraint modes and the interface normal modes. Constraint modes and interface normal modes together are referred to as component modes.

Since the algorithm relies on the component mode synthesis method, which is based on the modal analysis, only linear properties are considered during the formation of the modal neutral file. All geometric and physical nonlinearities are ignored. If significant geometric nonlinear effects are present in your component, you must subdivide the component into several smaller components and transfer each one separately. You can then assemble the subdivided components in MBS to form a flexible component with geometric nonlinearity

The parameters which influence the accuracy of the reduction are the number and location of the boundary nodes and the number of first modes considered during the reduction. These parameters can be validated, for example, by computing a modal analysis of the FE model with constrains in ANSYS and separately in ADAMS and by subsequent comparison of the results.

It is useful if the modal analysis of the flexible part is computed before the reduction. Results obtained from the modal analysis are natural frequencies and mode shapes of the flexible part. These results can be used for suitable reduction parameters. Figure 3 demonstrates natural frequencies and mode shapes of an in-line six-cylinder diesel engine crankshaft.
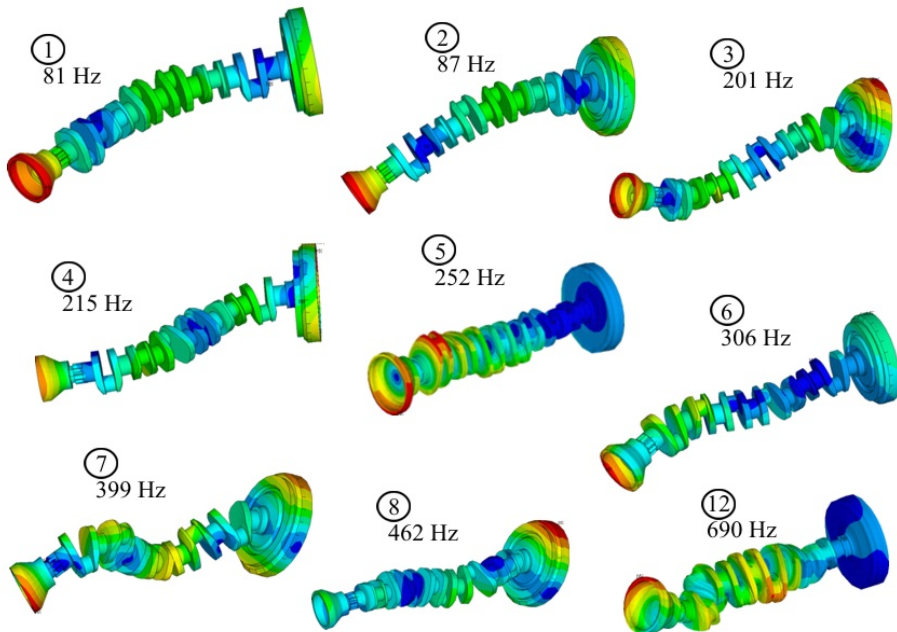


**Figure 3** Natural modes of in-line six-cylinder diesel engine crankshaft

The modal analysis results provide a very important step before dynamic solution in time domain. The fundamental first torsional mode shape is at 252 Hz and the second torsional mode shape is at 690 Hz. Only modes up to 2000 Hz are considered for the reduction.

## 2.2. Crankcase Stiffness Determination

Designers in the crankcase development process are constantly looking for ways to improve crankcase stiffness. The optimization of the crankcase design presents a crucial way for vibration and acoustic behavior improvement of the engine.

Crankcase stiffness also significantly influences cranktrain dynamics. As the stiffness of the crankcase is higher, the crankshaft vibrations are lower.  Mainly bending vibrations of the crankshaft are very sensitive on crankcase stiffness. Torsional vibrations of the crankshaft are partially influenced as well. If the stiffness is decreased then the torsional natural frequency raises up and vibrations decrease.

Figure 4 presents crankcase stiffness in each main bearing for two axes. Y-axis is parallel to the axis of cylinders.
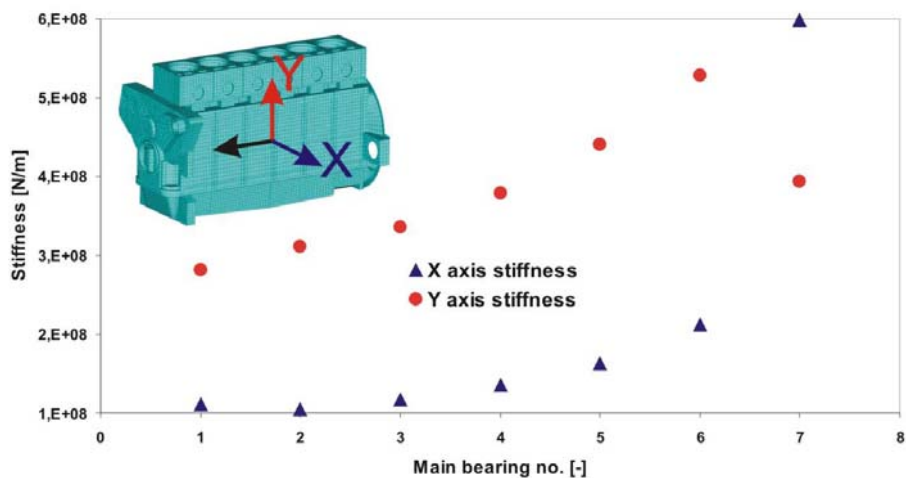


**Figure 4** Crankcase stiffness vs. main bearing No.

## 2.3.    Slide Bearing Model

A slide bearing is described as a sleeve around a pin with a lubricating fluid. The lubricant is supplied with a suitable slot. Tangential and radial motion, in combination with a wedged gap, generate a pressure in the oil film in the slide bearing. Bearing loading is periodical and a pin center comes through a bearing trajectory.

The dynamic behavior of hydrodynamic bearings is described by the Reynolds differential equation. The Reynolds differential equation cannot be solved analytically.

The three-dimensional method is used for the slide bearing model that includes misalignment effects. The Reynolds equation must be solved explicitly. To keep the simulation effort in a reasonable range, the hydrodynamic solution must be decoupled from the dynamic solution of MBS Solver. Therefore, the Reynolds equation is solved for several bearing working conditions (eccentricities and misalignment angles) prior to the dynamic analysis. The results are stored in hydrodynamic databases representing dimensionless bearing reactions (forces and force-attachment coordinates) to dimensionless states (eccentricity and misalignment value). During the dynamic solution, MBS Solver subroutines do the database access and the necessary analytical steps (coordinate transformations, and so on) [4].

## 2.4. Rubber Damper

A torsional damper is an essential part of most engines. Truck or tractor engines cannot generally work without the torsional damper because torsional vibrations in resonances are too dangerous for engine running. Two types of torsional dampers are applied most frequently: a rubber and a viscous-type vibration damper.

The rubber damper consists of a rubber band interposed between an outer inertia mass and a flange which is attached to the front end of the crankshaft. The rubber is vulcanized to both members. Rubber stiffness decreases with high deformation while its damping ability remains constant or even decreases. Likewise, heat reduces both the stiffness and the damping ability. Rubber has the ability to store enormous amounts of energy and can release most of this energy on retraction.

The main difference between a rubber damper and a viscous-type damper is that the viscous-type damper is untuned but is very capable of reducing the amplitude and smoothing out major critical orders. Consequently, the rubber damper has a natural frequency of its own, the value of which is chosen to detune major critical orders so that their vibrations occur at different speeds with much reduced amplitude.

## 2.5. Viscous-type torsional damper

The design of a damper consists of an annular-shaped flywheel enclosed in a light steel casing, which is rigidly attached to the crankshaft via a pulley wheel hub. The flywheel annular chamber is completely sealed by the side cover fitted into a recess machined on the exposed side of the casing which is rolled over. The flywheel has a radial clearance of about 0.25 mm and a lateral clearance of up to 0.5 mm in the chamber and the existing space between the flywheel and casing walls is fitted with a very viscous silicone fluid that changes little with temperature.

If there is very little or no vibration at the end of the crankshaft, the viscous torque drag causes the annular damper mass to rotate with the casing. If the damper casing is suddenly rotated, the flywheel will move only so far as it is dragged by the fluid, and if the direction of rotation is reversed, the flywheel will overrun before it is itself reversed. Consequently, with rapid and continual changing of direction during a torsional vibration the fluid in the case is being sheared and it is the resistance to this shearing action which forms the damping force. Thus, when the frequency and amplitude of the oscillations cause the vibration torque acting on the damper mass to exceed the viscous torque, a relative slip occurs. It is slippage between the casing and flywheel, which is responsible for the absorption of vibratory energy which is simultaneously dissipated in the form of heat to the surroundings.

## 3. Solution in ADAMS

The solution of the complex model in time domain runs in ADAMS. Major parts, for example a crankshaft, are solved as flexible parts. The other parts are solved as rigid. Gas forces on pistons and a torsional damper are added in ADAMS as well. Some temperature elements for the dependency on temperature are defined. The first

temperature element defines the dependency of oil temperature in bearings on the engine speed, and is referenced by a viscosity element that describes the dependency of oil viscosity on oil temperature. The oil viscosity is then necessary to describe the behavior of hydrodynamic bearings. The second temperature element defines the dependency of the torsional vibration damper temperature on the engine speed, which is referenced again by the torsional damper.

The solution is very complicated and requires a great deal of computer time. The numerical solution of the equation of the motion in time domain is solved using Newmark method with integration time step corresponding to a crank angular displacement of approximately 0.01°.

## 4. Measurement technique

The comparison of calculations and measurements is still a decisive quality criterion in the CAE environment. Non-contact measurements with laser Doppler vibration meters enable verification of complex calculation models. The torsional vibration meter B&K Type 2523 (see Figure 5) was designed for making torsional vibration measurements in places where mounting a transducer onto a rotating object is not possible.



**Figure 5** Laser torsional vibration meter B&K Type 2523 (left) and Laser vibration meter B&K Type 3544 (right)

The laser torsional vibration meter, its principles and applications are described below. A schematic diagram of the electronic and optical components in the torsional vibration meter is shown in Figure 6.
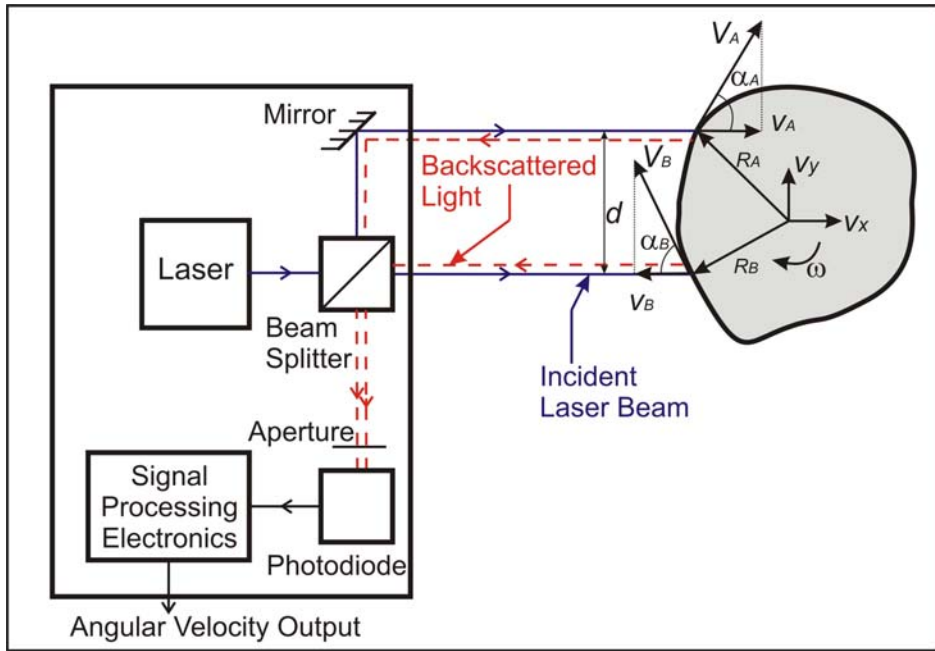
**Figure 6** The arrangement of the electronic and optical components
within the B&K Type 2523

The central module of the system is a low power Ga-Al-As laser. The laser beam is split into two equal-intensity parallel beams separated by a distance

$$d = R_A \cos\alpha_A + R_A \cos\alpha_B \quad . \tag{1}$$

The beams strike the shaft surface at points A and B, where the velocity is $V_A$ and $V_B$, respectively. Each beam sees only the velocity in the x-direction

$$v_A = -V_A \cos\alpha_A - V_x = -\omega R_A \cos\alpha_A - V_x \tag{2}$$

$$v_B = V_B \cos\alpha_B - V_x = \omega R_B \cos\alpha_B - V_x \tag{3}$$

and is thus frequency-shifted

$$f_A = \frac{2v_A}{\lambda} \quad \text{and} \quad f_B = \frac{2v_B}{\lambda} \tag{4}$$

The returning beams then heterodyne, giving an output current modulated at the beat frequency, $f_D$, a.i., the difference between the frequencies of the Doppler-shifted beams

$$f_D = f_B - f_A = \frac{2}{\lambda}(v_B - v_A) = \frac{2\omega d}{\lambda}$$

(5)

Thus, the beat frequency is directly proportional to the shaft speed $\omega$ and is independent of any solid body motion ($V_X + V_Y$) of the shaft. If the plane of the laser beams is not perpendicular to the shaft axis, then $f_D$ is also a function of $\cos \Phi$, where $\Phi$ is the angle between the plane of the laser beams and the plane perpendicular to the axis of shaft rotation.
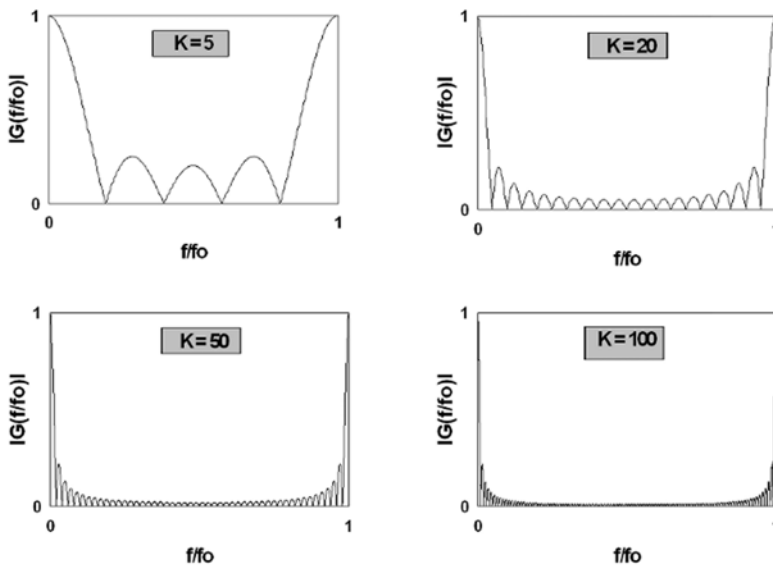


**Figure 7** Filter characteristics

The torsional vibrations of the six-cylinder in-line diesel engine have been measured and evaluated by in-house software. The measured signal has been processed by the averaging filter

$$y(t) = \frac{1}{K} \sum_{k=0}^{K-1} x(t - kT)$$

(6)

whose characteristic

$$G\left(\frac{f}{f_0}+i\right)=G\left(\frac{f}{f_0}\right)=\frac{1}{K}\left|\frac{\sin\left(K\pi\frac{f}{f_0}\right)}{\sin\left(\pi\frac{f}{f_0}\right)}\right|, \quad i=1,2,\ldots \qquad (7)$$

is periodical. For filter characteristics see Figure 7.

## 5. Diesel in-line six-cylinder engine results

Failures and mainly fatigue fractures occurred with an engine power increase and material savings in the past. These fractures were not caused only by forces from combustion pressure processes and inertial forces or incorrect construction but it was found that the main portion of these fractures was caused by periodical torsional vibrations of the crankshaft. Three types of crankshaft vibrations exist in agreement with traditional approach: bending, torsional and axial vibrations. Bending vibrations are caused by periodical forces that operate perpendicular on the crankshaft axis. These forces are radial and tangential forces on the crankshaft and imbalanced eccentric forces of the cranktrain. Natural frequencies of bending modes are given a free length of the crankshaft between the bearings. Free lengths of crankshaft between two bearings are very small and natural frequencies of bending modes are high and there are no resonances at an engine speed range. Stiffness of the bearings and the engine block has a large influence on bending natural frequencies.

Torsional vibrations of crankshafts are much more dangerous than bending vibrations. Forced torsional vibrations of the crankshaft are caused by time depended torques. Torsional vibrations reach high values in resonances when the frequency of forced vibration is equal to natural frequency. The resonances and relevant critical engine speeds cause an increased noise and engine vibrations. All vibration types can be obtained from a complex computational model of the cranktrain [1].

The complex computational model of the in-line six-cylinder diesel engine was developed and verified by measurement on an experimental engine with attached Schenck dynamometer type W 400. Figure 8 shows the placement of the laser torsional vibration meter B&K Type 2523 for the measurement of crankshaft pulley torsional vibrations.
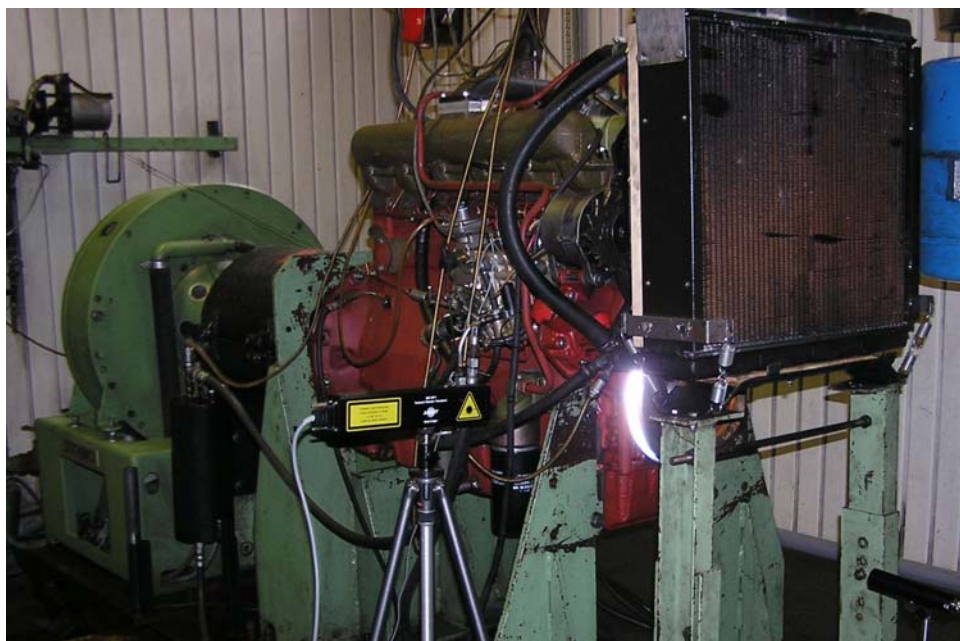
**Figure 8** In-line six-cylinder diesel engine measurement with help of laser torsional vibration meter B&K Type 2523

The opening analysis of cranktrain dynamics is a modal analysis. Natural frequencies and mode shapes of the cranktrain are found. The first torsional natural frequency has the greatest effect on torsional forced damped vibrations and in the case of analyzed engine occurs at 238 Hz. The second torsional natural frequency occurs at 640 Hz, has only a smaller effect and is included in the forced damped solution. Critical engine speeds can be determined from the first torsional natural frequency and dominant harmonic orders.

Table 1 presents computed and measured natural frequencies of the in-line six-cylinder engine cranktrain without a torsional damper. Bending vibration modes cannot be directly measured with laser vibration meters and therefore measured bending natural frequencies are not presented in the table.

| Natural freq. No. | Natural freq. | Natural freq. | Mode shape |
|:---:|:---:|:---:|:---:|
| [-] | [Hz] | [Hz] | description |
| | Computation | Measurement | |
| 1 | 208 | - | bending |
| 2 | 238 | 237 | torsion |
| 3 | 267 | - | bending |
| 4 | 289 | - | bending |
| 5 | 300 | 292 | axial |
| 6 | 319 | - | bending |

**Table 1** Natural frequencies of in-line six-cylinder engine cranktrain.

Critical engine speeds can be determined from the first torsional natural frequency and engine dominant orders (see Table 2). An engine firing order is 153624 and the critical orders acting in the engine speed range are the $12^{th}$, $9^{th}$, $7.5^{th}$, $6.5^{th}$ and $6^{th}$.

| Diesel in-line 6-cylinder cranktrain | | |
|---|---|---|
| Order | Computation | Measurement |
| $\kappa$ | $n_{CRIT}$ | $n_{CRIT\_E}$ |
| [–] | [min$^{-1}$] | [min$^{-1}$] |
| 3 | 4800 | 4740 |
| 6 | 2400 | 2370 |
| 6,5 | 2215 | 2188 |
| 7,5 | 1920 | 1896 |
| 9 | 1600 | 1580 |
| 12 | 1200 | 1185 |

**Table 2** Critical engine speeds

Computed and measured forced torsional vibrations of the cranktrain without a damper vs. the crank angle are presented in Figure 9.
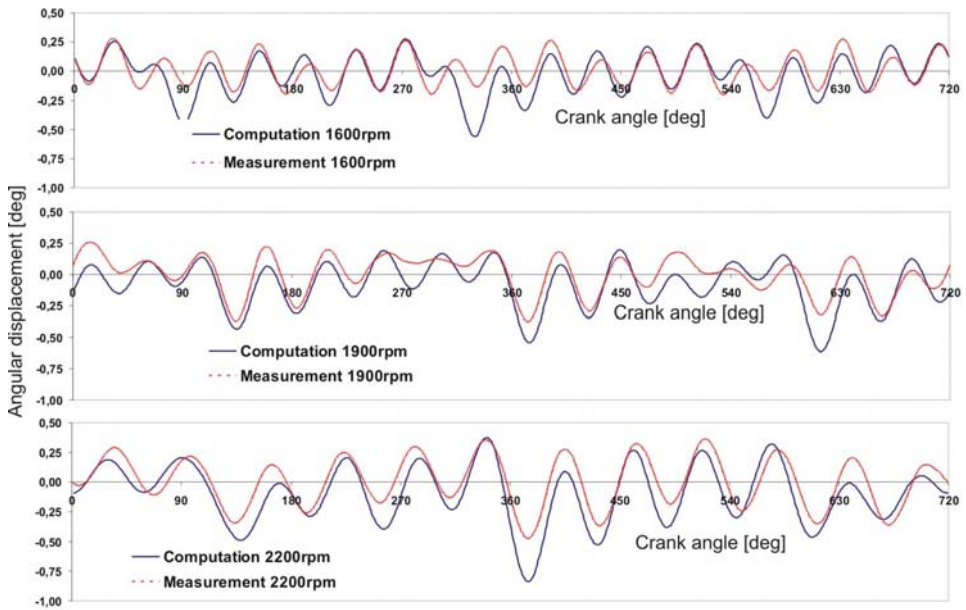


**Figure 9** Computed and measured torsional vibrations vs. crank angle

Engine speeds presented in Figure 9 are chosen for resonances of the $7.5^{th}$, $9^{th}$ and $6.5^{th}$ orders. The engine speed of 2380 rpm (the $6^{th}$ order resonance) could not be verified because a crankshaft damage may have occurred.

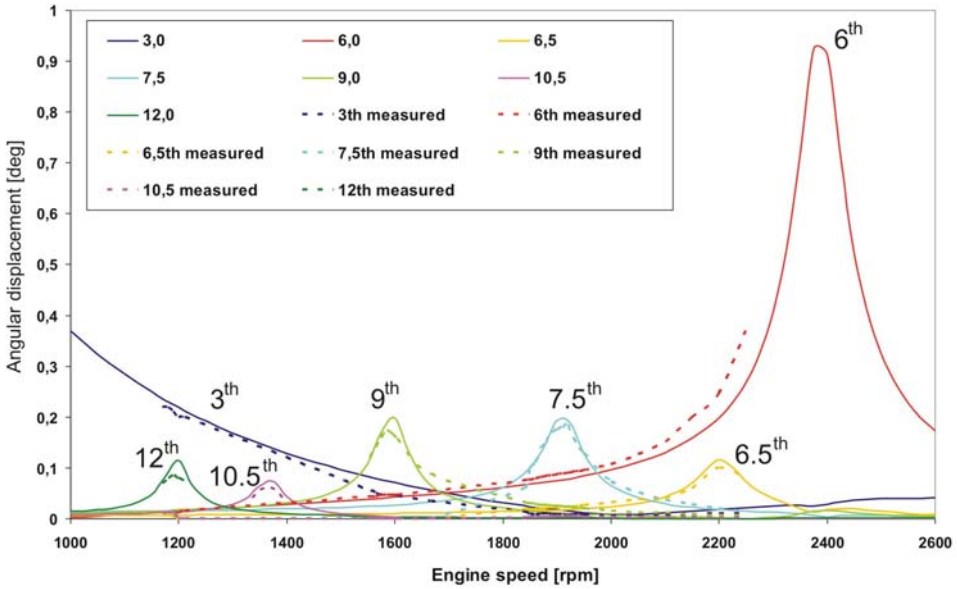Computed and measured engine dominant order amplitudes are shown in Figure 10.



**Figure 10** Computed and measured pulley torsional vibrations – single order amplitudes
without damper

Other critical orders can also be found with the engine speed range for six-cylinder with firing order 153624. These orders are the $5.5^{th}$, $4.5^{th}$, $3.5^{th}$, $3^{rd}$ and $2.5^{th}$ and again all orders for the second torsional natural frequency. Generally, the third or fourth torsional natural frequencies can cause problems as well but these may occur only for huge engines.

A six-cylinder crankshaft stress level roughly answers to the torsion moments acting on each crankthrow. The highest values of the torsion moment act on the $6^{th}$ crankthrow and higher stress can be expected on this crankthrow in critical engine speeds. The front end of the crankshaft includes gear assembly that drives the valvetrain. High torsional vibrations can cause timing problems of the valvetrain and have to be removed as much as possible. A much more critical scenario is a failure of the crankshaft due to fatigue.

Truck or tractor engines cannot generally work without the torsional damper because torsional vibrations in resonances are too dangerous for engine running. Two types of torsional dampers are applied – a rubber damper and a viscous-type damper.

The torsional vibration order analyses of the pulley of the in-line six-cylinder diesel engine without a damper, with a viscous-type damper and with a rubber damper are presented in Figure 11. It is evident that the viscous-type damper as well as the rubber damper eliminates all resonances in engine speed range from 1000rpm – to 2400rpm. Generally, the dampers ensure a decrease in the torsional natural frequencies. This

effect can be demonstrated on a cranktrain with a rubber damper where the $6^{th}$ order resonance for the second torsional natural frequency occurs at an engine speed of 2550 rpm.
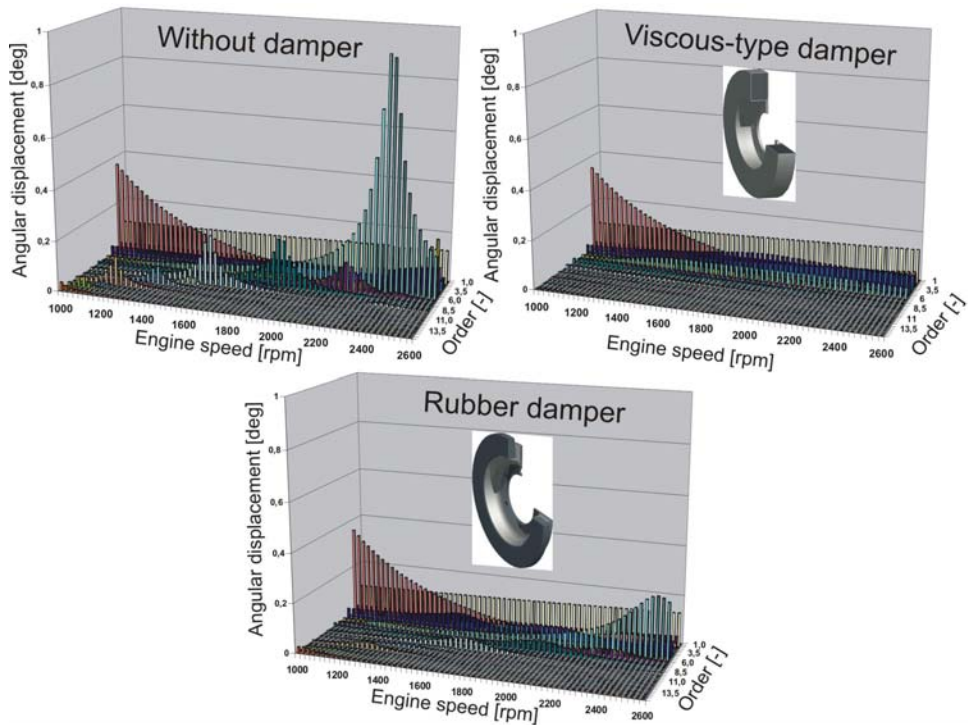


**Figure 11** Computed torsional vibration order analyses of in-line six-cylinder diesel engine pulley without damper, with viscous-type damper and with rubber damper

An axial displacement of the crankshaft pulley is another important section of the results and the computation results and measurements are focused on the pulley axial displacement in detail too.

Several components of the axial displacement of the crankshaft pulley exist. An axial bearing displacement is the first component. An oil film in the bearing is created at the start of the engine and this causes the axial displacement increase. After this, the axial bearing moves periodically within the range of an axial clearance. This component presents a smaller value of the total pulley axial displacement in the case of the in-line six-cylinder diesel engine. Longitudinal vibrations of the crankshaft are the second component of the total pulley axial displacement. The crankshaft axial displacement increases in engine speeds where some axial resonances exist, and presents a major component of total pulley axial displacement. The displacement of an

entire engine is the last relevant component of the pulley axial displacement and represents only a very small value. This component depends on the stiffness and damping of engine mounts.

Figure 12 shows the computed longitudinal vibration order analysis of the in-line six-cylinder engine crankshaft without a torsional vibration damper, with the viscous-type damper and with the rubber damper.
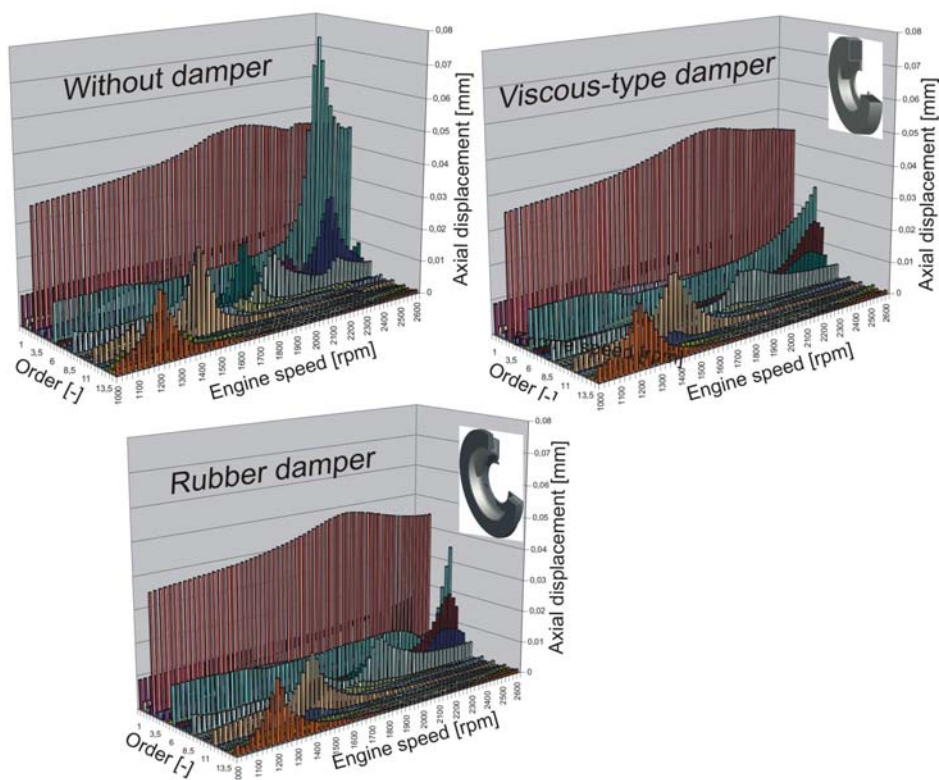


**Figure 12** Computed longitudinal vibration order analysis of in-line six-cylinder engine crankshaft without a torsional vibration damper

Other problems that can be solved by a complex cranktrain model are orbital displacements of main bearings or the displacement of the axial bearing. Main bearing journal centre orbital displacements are presented in Figure 13.
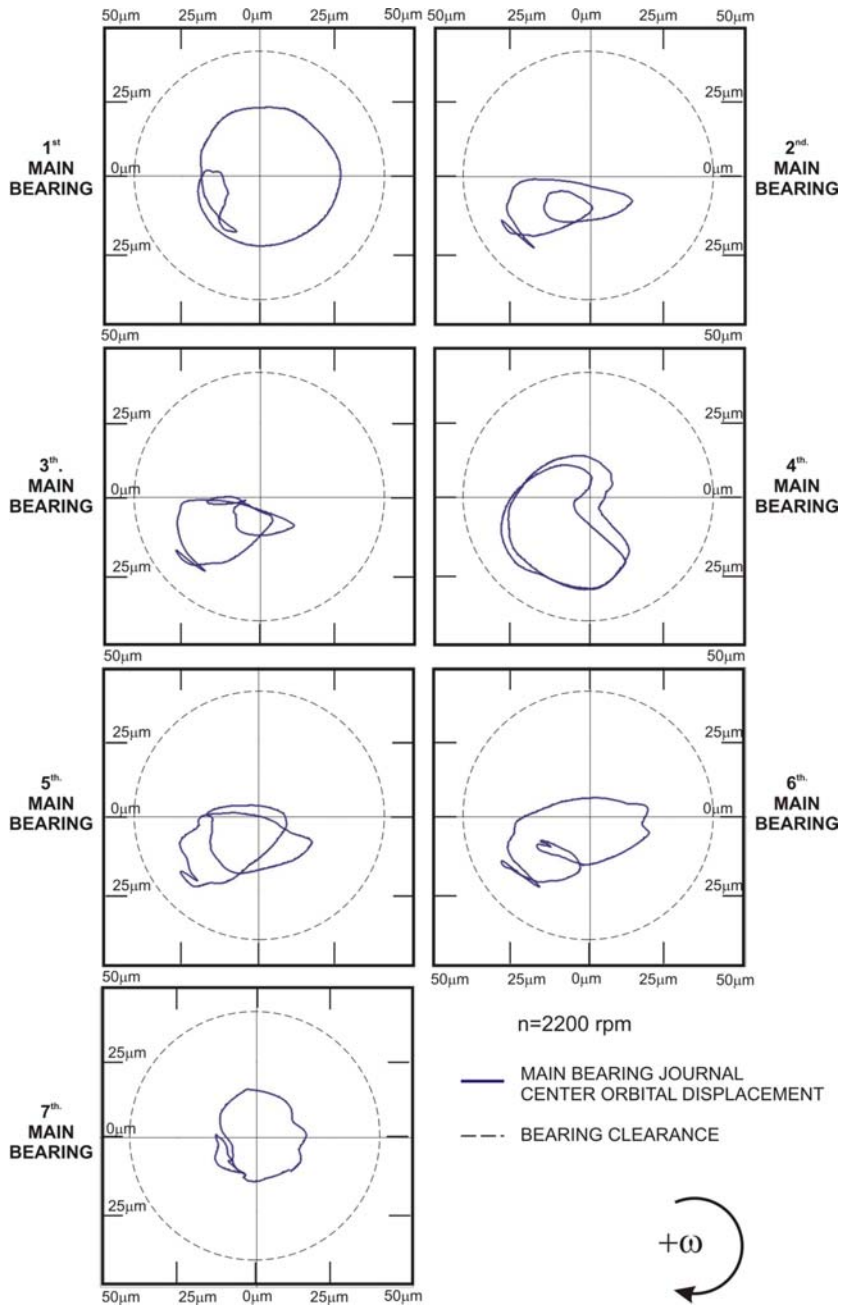
**Figure 13** Main bearing journal center orbital displacements

## 6.  Fatigue analysis

As a part of the engineering design process, engineers have to assess not only how the design satisfies the performance requirements but also how durable the product will be over its life cycle. A major cause of failure is the growth of cracks that grow due to fatigue loadings to the point where the product fails. This part describes an approach to predicting fatigue life and combines FEM and MBS systems.

Engine performance has to be kept for the whole engine service and therefore the decisive criterion for the most stressed parts is the fatigue analysis.

Fatigue calculations of a dynamically loaded crankshaft of an in-line six-cylinder diesel engine are carried out on the basis of finite element calculation results.

The calculation methods used for the assessment of FE results are based on experimental and theoretical research results, model trials and operational experience.

The starting point for the multi axial-fatigue analysis is a time series of stress tensors for a specific node. Critical cutting plane methods and material sensitive equivalent stress hypotheses are used to count rainflow matrices. Damage is computed from the rainflow matrices taking many fatigue influences into account (notches, mean stress, temperature etc.)

The basic procedure is based on the influencing quantity methods described in the TGL and the new FKM guidelines (Dannbauer, 2004). On the basis of strength data from unnotched samples, local S/N curves are calculated at FE nodes which are influenced by local component properties and loads.

The influence of notches on the component strength, for example, requires special solutions in the FE modeling. Since the classical route using notch form factors is not available because of a lack of nominal cross-sections, a method based on load gradients and material properties is applied.

High cycle fatigue can be expressed by using endurance safety factors. The endurance limit safety factor can be defined as

$$SF = \frac{\sigma_A + \sigma_m}{\sigma_a + \sigma_m},$$

(8)

where    $\sigma_A$    allowable amplitude,

$\sigma_M$    mean stress,

$\sigma_a$    actual occurring amplitude.

A minimum endurance limit safety factor (MSF) is the minimum value of all endurance limit safety factors of the FEM model and can be expressed as

$$MSF = \min\{SF_i\}.$$

(9)

A minimum endurance limit safety factor of e.g. MSF = 1.2 with regard to the upper stress is interpreted so that one could increase the total stress (amplitude + mean

stress + possible constant stress) by a factor of 1.2 in order to achieve an endurance limit safety factor of MSF = 1.0, all other things being equal.

Crankshaft surface distribution of endurance safety factors in Figure 14 is presented for a crankshaft without a torsional vibration damper and for the engine speed of 2200 rpm.
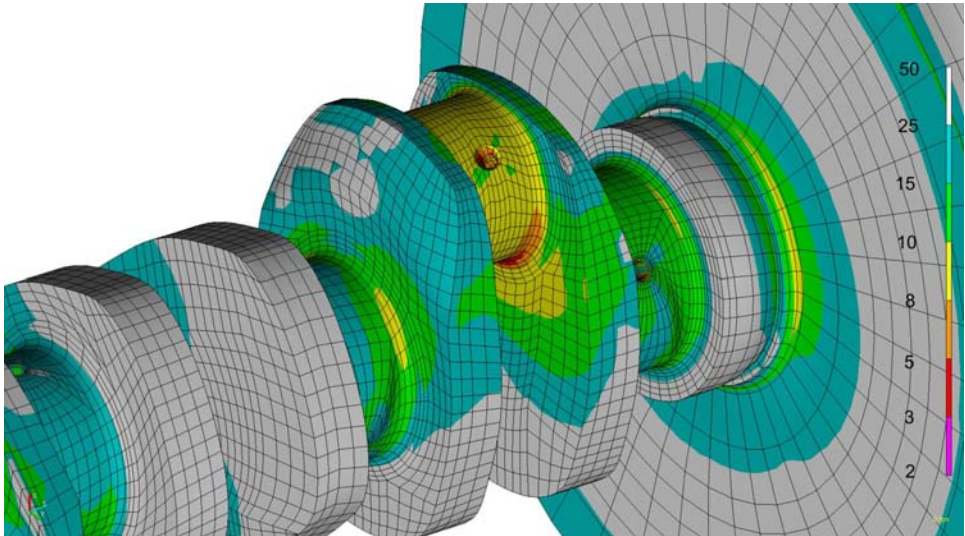


**Figure 14** Critical spots of endurance safety factors of crankshaft

A minimum value of the endurance safety factor of a crankshaft without a damper belongs to resonance of the 6th harmonic order (2400 rpm) on the sixth crank throw. The local minimum values at engine speeds of 1200rpm, 1600rpm and 1900rpm belong to torsional resonances of the 12th, 9th and 7.5th orders. Minimum safety factor less than 1 is at the engine speed of 2400rpm and a crankshaft failure would occur during the engine life. Applications of the torsional damper increase crankshaft fatigue into safety limits.

The minimum endurance limit safety factor of the crankshaft against the engine speed is shown in Figure 15. This figure demonstrates the influence of a torsional damper on minimum endurance limit safety factors of the crankshaft.
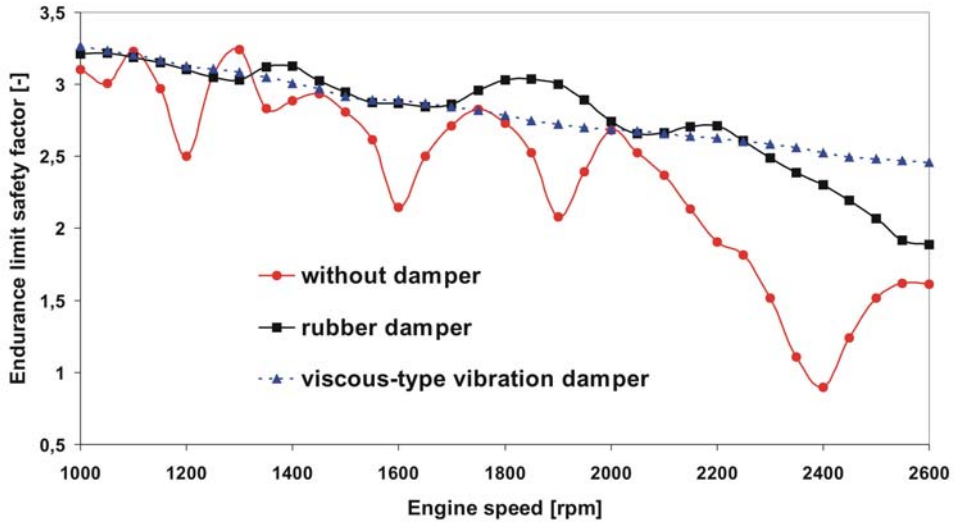
**Figure 15** Crankshaft minimum endurance limit safety factors vs. engine speed

Applied viscous torsional vibration dampers with extremely high viscosity silicone fluids and rubber dampers are effective means of modern engine vibration and noise reduction and significant fatigue increases.

## 7. Conclusion

The virtual prototype of the cranktrain can study and refine real-world engine performances. These are often multiphysics analyses for studying the interaction of all factors encountered throughout the overall engine development, including real-world factors that radically influence performance such as temperature, fluid flow, vibration, and fatigue. Such simulation may determine the deformation of the crankshaft and connecting rods, for example. This approach overcomes the historic "build-test-redesign" problems by evaluating designs through computer simulation and analysis earlier in the product development process and reducing reliance on validation testing late in the cycle. Common performance problems that are encountered late in the product development cycle necessitate repetitive redesign cycles until satisfactory performance is achieved, with several testing iterations usually required. This adds considerable time and cost to the military truck development cycle.

The presented virtual cranktrain development provides a powerful implement and in combination with the Laser measuring technique with special in-house software is an efficient way for truck engine development.

## Acknowledgement

R e f e r e n c e s :

[1] NOVOTNÝ, P.: Cranktrain dynamics simulation – central module of virtual engine, Ph.D.Thesis, Brno University of Technology, Brno 2005, ISSN 1213-4198

[2] PÍŠTĚK, V., NOVOTNÝ, P.: Multi-Body Analysis of Diesel Engine Dynamics, XXXV. Mezinárodní konference kateder a pracovišť spalovacích motorů českých a slovenských vysokých škol, MZLU v Brně 2004, ISBN 80-7157-776-6 (pp. 23-29)

[3] PÍŠTĚK, V., NOVOTNÝ, P.: Virtual Engine - A Tool for Reliability Increase. In Reliability 2004, University of Defence in Brno, 12th – 14th October 2003

[4] REBBERT, M.: Simulation der Kurbewellendynamik unter Berücksichtigung der hydrodynamischen Lagerung zur Losung motorakusticher Fragen. Ph.D. Thesis. Fakultät fur Maschinenwesen der Rhenisch-Westfalishen Technischen Hochschule Aachen, Januars 2000

[5] SHABANA, A.: Dynamic of Multibody System – Second Edition. Cambridge University Press, Cambridge, United Kingdom, 1998. ISBN 0 521 594464

[6] STODOLA, J.: State-of-the-Art Automotive Lubricants. Transport Means 2005 Kaunas Lithuania, 2005 ISSN 1822-296 X ((pp 37 – 40)